ARIA Is Concentrated in the Synaptic Basal Lamina of the Developing Chick Neuromuscular Junction

Andrew D. J. Goodearl, Ann G. Yee, Alfred W. Sandrock Jr., Gabriel Corfas, and Gerald D. Fischbach

Neurobiology Department, Harvard Medical School, Boston, Massachusetts 02115

Abstract. ARIA is a member of a family of polypeptide growth and differentiation factors that also includes glial growth factor (GGF), neu differentiation factor, and heregulin. ARIA mRNA is expressed in all cholinergic neurons of the central nervous systems of rats and chicks, including spinal cord motor neurons. In vitro, ARIA elevates the rate of acetylcholine receptor incorporation into the plasma membrane of primary cultures of chick myotubes. To study whether ARIA may regulate the synthesis of junctional synaptic acetylcholine receptors in chick embryos, we have developed riboprobes and polyclonal antibody reagents that recognize isoforms of ARIA that include an amino-terminal immunoglobulin C2 domain and examined the expression and distribution of ARIA in motor neurons and at the neuromuscular junction. We detected significant ARIA mRNA expression in motor neurons as early as embryonic day 5, around the time that motor axons are making initial synaptic contacts with their target muscle cells. In older embryos and postnatal animals, we found ARIA protein concentrated in the synaptic cleft at neuromuscular junctions, consistent with transport down motor axons and release at nerve terminals. At high resolution using immunoelectron microscopy, we detected ARIA immunoreactivity exclusively in the synaptic basal lamina in a pattern consistent with binding to synapse specific components on the presynaptic side of the basal lamina. These results support a role for ARIA as a trophic factor released by motor neuron terminals that may regulate the formation of mature neuromuscular synapses.

We have been studying certain trophic interactions between motor neurons and muscle cells at embryonic neuromuscular junctions (nmjs)[1] to understand how synapse formation is regulated. The embryonic chick was used in these studies, as this system is accessible to experimental manipulation, the procedures for culturing nerve and muscle cells are well established and events in synapse development are well characterized. In the chick hind limb, advancing motor neuron growth cones first enter the unsegmented muscle masses at embryonic day 4-5 (E4-5) (Bennett et al., 1980; Tosney and Landmesser, 1985), a time when mononuclear myoblast cells are fusing to form myotubes (Bonner and Hauschka, 1974). Elementary neuromuscular synapses have been detected on embryonic day 6, by measurement of nerve-evoked muscle activity (Landmesser and Morris, 1975) and of synaptic potentials (Landmesser, 1978) and the accumulation of acetylcholine receptors (AChRs) at endplates (Smith and Slater, 1983; Fallon and Gelfman, 1989). Further specialization of the nmj continues throughout embryonic life and posthatching (E21) including the capping of nerve terminals by nonmyelinating perisynaptic Schwann cells, the assembly of specific components into a thickened synaptic basal lamina beneath nerve terminals and capping Schwann cell, and the nerve-dependent reduction of extrasynaptic AChR density (for recent review see Hall and Sanes, 1993).

An essential event of synaptic specialization is the concentration of acetylcholine (ACh) receptors on nascent myotubes and on myoblasts, in the vicinity of ingrowing motor neuron growth cones. This effect has been observed in vitro in cocultures, where "hotspots" of ACh sensitivity were detected where motor neurons contacted myotubes (Frank and Fischbach, 1979). Medium conditioned by motor neurons can also stimulate increased ACh receptor incorporation into the surface of cultured myotubes (Corfas et al., 1993). It is likely, therefore, that one or more neuron-derived trophic factors plays a role in forming and maintaining high concentrations of AChRs at nmjs. One such factor is agrin, a 210-kD protein that causes the aggregation of preexisting muscle AChRs into clusters in vitro. Agrin is transported down motor axons and released at nerve terminals in vivo and may stimulate the formation

Address correspondence to Dr. G. D. Fischbach, Neurobiology Department, Harvard Medical School, 220 Longwood Ave., Boston, MA 02115. Tel.: (617) 432-2510. Fax: (617) 432-3223.

1. *Abbreviations used in this paper*: ACh, acetylcholine; AChR, acetylcholine receptor; ARIA, acetylcholine receptor inducing activity; ALD, anterior latissimus dorsi muscle; GGF, glial growth factor; nmj, neuromuscular junction; HSPGs, heparan sulfate proteoglycans; KLH, keyhole limpet hemocyanin; NFDM, nonfat dried milk; nmjs, neuromuscular junctions.

of dense cytoskeleton-associated receptor patches beneath nerve terminals (Reist et al., 1992; Fallon and Hall, 1994). Regulation of the rates of AChR synthesis and insertion into the plasma membrane is less well understood. These effects might be mediated by acetylcholine receptor inducing activity (ARIA), a 42-kD protein found in extracts of chick brain. ARIA purified from adult chick brains: (*a*) specifically increases the rate of insertion of newly synthesized receptors into the plasma membrane of cultured myotubes (Usdin and Fischbach, 1986; Dubinsky et al., 1989); (*b*) causes the elevation of AChR α (2–16-fold) and ϵ (10-fold) subunit mRNA levels in vitro (Harris et al., 1988; Martinou et al., 1991); and (*c*) increases expression of myotube sodium channels that are also found concentrated at nmjs (Corfas and Fischbach, 1993).

We recently purified ARIA to homogeneity and cloned a corresponding cDNA, named clone λ12, from an E19 chick spinal cord library (Falls et al., 1993). The cDNA sequence suggests that ARIA is synthesized as an intrinsic membrane precursor protein with a single transmembrane segment linking an NH_2-terminal extracellular domain and a COOH-terminal cytoplasmic domain. The extracellular region contains consensus *N*- and *O*-glycosylation sites, an Ig C2-like domain, an EGF-like domain and a dibasic motif adjacent to the transmembrane sequence that may mediate proteolytic release from the membrane surface.

Sequence comparison reveals that ARIA is a member of a family of growth factors that includes glial growth factors (GGFs) that stimulate Schwann cell proliferation (Goodearl et al., 1993; Marchionni et al., 1993), and neu differentiation factor and heregulin that effect proliferation or differentiation in diverse mammary tumor cell lines (Holmes et al., 1992; Wen et al., 1992). Nucleic acid sequence comparisons show that these cDNAs are derived from a single gene that may generate in excess of 15 isoforms through alternative splicing (Marchionni et al., 1993; Wen et al., 1994). A common structural feature of isoforms active in the above assays is the presence of the EGF-like domain. Indeed, this domain alone gives rise to all of the observed bioactivities (Holmes et al., 1992; Goodearl, A. D., D. L. Falls, and G. D. Fischbach, unpublished results). In situ hybridization analysis has shown high levels of ARIA mRNA in all cholinergic neurons in the adult CNS, including motor neurons (Corfas et al., 1995). It is also found in the cerebellum, in sensory ganglia and in nonneural tissues such as the heart.

Given its biological properties, its predicted molecular structure and the high levels of expression in motor neurons, ARIA is an excellent candidate for trophic function. Further, we hypothesize that ARIA is expressed by motor neurons at the time that synapses form and that ARIA protein is present at the neuromuscular junction to exert its trophic effects. In this study, we tested this hypothesis by examining the expression of ARIA mRNA in developing motor neurons and determining the location of ARIA protein at embryonic nmjs using light microscopy. We also used immunoelectron microscopy to determine the precise location of ARIA at nerve terminals as several laboratories have reported an activity associated with synaptic basal lamina that increases the rate of AChR synthesis in adult muscle (Burden et al., 1979; Goldman et al., 1991; Brenner et al., 1992; Jo and Burden, 1992). We observed that ARIA mRNAs are present in motor neurons at the earliest time that clusters of AChRs have been observed (E5) and continue to be expressed throughout development. In E18 embryos, ARIA protein is clearly evident at nmjs, consistent with axonal transport and release by nerve terminals. ARIA was concentrated in the thickened basal lamina throughout the synaptic zone in a pattern reflecting entrapment of secreted ARIA through specific interactions with basal lamina molecules. ARIA immunoreactivity was not detected before E16. Rapid accumulation soon thereafter suggests an event, perhaps binding in the synaptic cleft, that plays a role in the maturation and maintenance of nmjs.

Materials and Methods

In Situ Hybridization

In situ hybridizations were performed as previously described (Falls et al., 1993; Sassoon and Rosenthal, 1993). Tissues were fixed by immersion in 4% paraformaldehyde in PBS overnight at 4°C. After fixation, tissues were slowly dehydrated and embedded in paraffin. Serial transverse sections (9 μm) were collected on gelatinized glass microscope slides. Hybridization with sense and antisense probes was carried out at 52°C for 18 h in 50% deionized formamide, 0.3 M sodium chloride, 20 mM Tris-HCl pH 7.4, 5 mM EDTA, 10 mM $NaPO_4$ (pH 8), 10% dextran sulfate, 1× Denhardt's solution, 50 μg/ml total yeast RNA with 3.5×10^4 cpm/μl ^{35}S-labeled RNA probe under siliconized coverslips. After hybridizations, coverslips were floated off in 5× SSC, 10 mM dithiothreitol at 50°C, and washed in 50% formamide, 2× SSC, 10 mM dithiothreitol at 65°C. Slides were then rinsed in washing buffer, treated with RNAse A (20 μg/ml, Sigma Chem. Co., St. Louis, MO), and washed at 37°C for 15 min in 2× SSC and then for 15 min in 0.1× SSC. Sections were dehydrated rapidly, processed for autoradiography using NTB-2 Kodak emulsion, exposed for 1 or 2 wk at 4°C, and examined using both light- and dark-field illumination (Darklite; MVI, Avon, MA) under a dissecting microscope (SMZ-U; Nikon, Japan). The templates for probe transcription used in this study corresponded to the 5′ 82 bp or 337 bp of ARIA clone λ12. Sense and antisense RNA probes, labeled with [^{35}S]UTP (>1,000 Ci/mmol; New England Nuclear, Boston, MA), were generated by runoff transcription of the restriction digested plasmid using T7 or SP6 RNA polymerase. Transcripts were degraded to an average length of 110 bp using alkaline hydrolysis (Sassoon and Rosenthal, 1993).

Preparation of Anti-ARIA (HM22) Antiserum

A 28–amino acid peptide was synthesized (peptide synthesizer 430A; Applied Biosystems, Inc., Foster City, CA; Fmoc chemistry) using the NH_2-terminal 27 residues predicted from the chick proARIA1 λ12 cDNA sequence (MWATSEGPLQYSLAPTQTDVNSSYSTV) with an additional COOH-terminal cysteine. A saturated solution of this partially soluble peptide was conjugated with keyhole limpet hemocyanin (KLH) using the cross-linking reagent sulpho-MBS (Pierce Chem. Co., Rockford, IL) according to the manufacturers instructions. After desalting the sample by gel filtration on a PD-10 column (Bio-Rad Labs., Richmond, CA) and lyophilization, two rabbits were inoculated with 100 μg of peptide/KLH conjugate followed by monthly boosts of 50 μg (Cocalico Biologicals, Reamstown, PA). Weekly bleeds were screened by ELISA using peptide coated plates. Serum from the rabbit with the highest titer (HM22) was affinity purified over a peptide/ovalbumin/Sepharose affinity column in 10 mM Tris-HCl, pH 7.4. After extensive washing of the column in 0.5 M NaCl, 10 mM Tris, pH 7.4, a 0.1 M Glycine, pH 2.5 step was used to elute fractions containing one-tenth volume 0.4% NaN_3, 1.0 M Tris, pH 8.0. Titer and purity of eluted fractions were monitored by ELISA and reducing SDS-PAGE respectively. High titer fractions were pooled, aliquoted and stored at 4°C. All experiments in this study were carried out with affinity-purified HM22 antiserum.

Immunohistochemistry

Anterior latissimus dorsi (ALD) muscles from embryonic chicks were im-

mersion fixed in 4% paraformaldehyde/PBS (pH 10) for 4 h before equilibration to 15% and then 30% sucrose solutions in PBS. 10–15-μm sections, prepared from frozen OCT-embedded tissues on a cryostat at −18°C, were thaw mounted on to Superfrost Plus slides (Fisher Scientific, Pittsburgh, PA). After being washed in PBS, the sections were permeabilized and blocked for 30–60 min in 0.4% Triton X-100, 10% normal goat serum (NGS), 0.1 M sodium phosphate, 0.5 M NaCl, pH 7.4. Sections were incubated overnight at room temperature in primary antibodies diluted in the same permeabilizing/blocking buffer. Sections were washed with PBS three times followed by a 1-h incubation in fluorescein or rhodamine conjugated secondary antibodies diluted in 3%NGS/PBS. When used, rhodamine-labeled α-bungarotoxin, prepared according to Ravdin and Axelrod (1977), was coincubated with the secondary antibodies at a dilution of 1:300. The sections were then washed three times with PBS and viewed under Citifluor (Ted Pella, Inc., Irvine, CA) on a fluorescence microscope (Microphot; Nikon Inc., Melville, NY) equipped with rhodamine and fluorescein optics. A third filter block (UV-1B, excitation 365 nm, barrier filter 400 nm) was used to observe autofluorescence that was not from fluorescein or rhodamine probes.

Electron Microscopy

For HRP labeling, the ALD muscles of E18 chick embryos were exposed and then rapidly immersion fixed in situ using 4% paraformaldehyde, 0.5% glutaraldehyde in 0.1 M Hepes, pH 7.4. After 30 min, the ALDs were dissected under fixative and fixed for an additional 30 min. After a PBS wash, muscle pieces were embedded in 5% agar in PBS and 75-μm vibratome sections were cut. These were blocked for 30–60 min in 10% NGS, 0.1 M sodium phosphate, 0.5 M NaCl, pH 7.4. Sections were incubated overnight in HM22 antibody diluted at 1:100 in blocking buffer. The primary antibody was omitted from some sections as a control. Sections were washed with PBS three times followed by a 1 h incubation with biotin-labeled goat anti–rabbit IgG in PBS. After a 10-min wash in PBS, sections were incubated in HRP-conjugated biotin complexed with avidin (Vector Labs., Inc., Burlingame, CA) for 1 h and washed once again in PBS for 10 min. The sections were then developed for 7 min in DAB peroxidase substrate solution (0.1% diaminobenzidine tetrahydrochloride, 0.02% hydrogen peroxide, 0.1 M Tris-HCl, pH 7.4) and washed in PBS. Sections were subsequently postfixed in 2% osmium tetroxide, 1.5% potassium ferrocyanide for 1 h followed by en bloc staining in 1% uranyl acetate, 0.1 M sodium maleate, pH 6.0. They were then dehydrated in a graded series of ethanols and embedded in epon/araldite. Silver-gray sections (65 nm) were cut on a Reichert Ultracut S and viewed in a Jeol 100CX electron microscope operated at 60 kV.

For the preparation of ultrathin cryosections (Tokuyasu, 1986), ALD muscles were immersion fixed in 8% paraformaldehyde, 1% glutaraldehyde, 0.6% picric acid in 0.1 M cacodylate, pH 7.4, for 1 h. The ALD muscle was dissected, washed in PBS, and cut into small blocks. The tissue was cryoprotected in 2.3 M sucrose for a minimum of 2 h and then rapidly frozen in liquid nitrogen. 70–80-nm sections were cut on a Reichert Ultracut S microtome equipped with an FCS freezing chamber. Sections were picked up on carbon-formvar–coated 200 mesh grids. Labeling of cryosections was performed according to the procedures of Slot and Geuze (1985). Briefly, sections were quenched in 0.02% glycine in PBS, pH 7.4, followed by 10 min in blocking solution (0.1% BSA in PBS). Grids were then incubated in primary antibody (HM22 diluted 1:100) for 35 min. After several rinses in blocking solution, grids were incubated in gold-labeled protein A for 30 min. Grids were again washed briefly in blocking buffer before several rinses in PBS for a total of 30 min. Grids were then fixed in 2% glutaraldehyde followed by a minimum of five 2-min washes in distilled water. Sections were then stained in 2% neutral uranyl acetate for 10 min and then stained for another 10 min in 1.8% methyl cellulose, 0.2% uranyl acetate. Grids were picked up in small wire loops, drained, and allowed to dry before viewing. For double labeling experiments, a mixture of HM22 and SV2 antibodies, both diluted at 1:100 in blocking buffer was used in the first incubation. Secondary antibody labeling was accomplished by mixing 10-nm gold-labeled goat anti–mouse IgG (diluted 1:40) with 5-nm protein A gold (diluted 1:60) and incubating the sections in this mixture for 30 min. The remaining steps were as for the HM22 single labeling experiments.

Antibodies

The anti-flag M2 monoclonal antibody (1:300) was from International Biotechnologies. The anti-neurofilament monoclonal antibody (clone NN18, 1:10), HRP-labeled goat anti–rabbit IgG (1:2,000) and HRP-labeled goat anti–mouse IgG (1:2,000) were from Boehringer Mannheim Corp. (Indianapolis, IN). Biotin-labeled goat anti–rabbit IgG (1:200) was from Vector Labs. Fluorescein-labeled goat anti–rabbit IgG (1:300) and rhodamine-labeled goat anti–mouse IgG (1:300) were from Cappel Labs. (Cochranville, PA). 10-nm gold-labeled goat anti–mouse IgG (1:40) was from Amersham Corp. (Arlington Heights, IL). 5- and 10-nm protein A gold (1:60) were from J. Slot (University Utrecht, Netherlands). SV2 hybridoma supernatant (1:100) was kindly donated by Dr. K. Buckley (Harvard Medical School).

COS Cell Transfection and Western Blotting

Two expression plasmids were prepared: p12.6, a control plasmid with the ARIA coding sequence in the antisense orientation (Falls et al., 1993) and EuFlag1, which encodes ARIA in the sense orientation with the following peptide sequence fused to the NH_2 terminus, MGDYYKDDDDKG-PVCWNSGVLRG, containing the flag epitope between residues 3 and 10 (Hopp et al., 1988). EuFlag1 was prepared by insertion of an oligonucleotide cassette into a BstX1 site in the polylinker of the proARIA1 expression construct p12.7 (Falls et al., 1993). COS-7 cells grown to 70% confluence in 100-mm tissue culture petri dishes were transfected with 10 μg of either EuFlag1 or p12.6 plasmids using the DEAE-dextran chloroquine method. After 48 h, all cells were harvested and pelleted by centrifugation. The pellets were resuspended in SDS-PAGE sample buffer with reducing agents and boiled for 5 min before electrophoresis in an 11% SDS–polyacrylamide gel. The protein bands were then electrophoretically transferred to an Immobilon membrane (Millipore Corp., Bedford, MA) in an electroblot apparatus (Bio-Rad) in 10 mM CAPS, 10% methanol pH11. Quantitative transfer was confirmed using prestained protein standards (Bio-Rad) run in the polyacrylamide gel. The blots were blocked in 5% nonfat dried milk (NFDM) in PBS overnight at 4°C. Replicate lanes in the same blot were incubated separately in three different primary antibody solutions diluted in 5% NFDM/PBS as follows: HM22 (1:100), HM22 (1:100) + 0.1 mg/ml peptide and αflag mAb M2 (1:300). After 2 h, each blot was washed four times for 5 min in PBS containing 0.1% Tween 20. The blots were then incubated for 1 h in either HRP-conjugated goat anti–rabbit IgG (HM22 blots), or HRP-conjugated goat anti–mouse IgG (M2 blot) diluted 1:2000 in 0.1% Tween 20/PBS. After being washed as above, the blots were developed in Renaissance chemiluminescence reagent (Dupont, Boston, MA) and exposed to autoradiography film.

Peptide Blocking Experiments

The peptide antigen was suspended at 1 mg/ml in PBS and agitated for 30 min to saturate the solution. Undissolved peptide was removed by centrifugation. HM22 antibody was diluted 1:10 in this peptide solution and agitated for a further 30 min. This solution was then diluted 1:10 either with the permeabilizing/blocking buffer for immunohistochemistry or with 5% NFDM/PBS for Western blot analysis.

Results

Expression of ARIA mRNA in Spinal Cord

In earlier studies, we demonstrated by Northern blotting that ARIA λ12 mRNA was expressed in the spinal cord and, by in situ hybridization, that the message was present in the ventral spinal cord of E7 chicks (Falls et al., 1993) when rudimentary neuromuscular connections have been formed. In this study, we examined whether ARIA expression was detectable earlier. Two antisense riboprobes were prepared, one 82-bp long and the other 337 bp long, which were specific for the coding sequence at the NH_2 terminus of the ARIA protein (20 and 105 amino acids, respectively, Fig. 1) plus a short 5′ untranslated sequence. In situ hybridization analysis of E5 chick embryos with each probe showed that ARIA λ12 mRNA was present and concentrated in the ventral horn of the spinal cord where motor neuron cell bodies reside (Fig. 2, *a* and *b*). There was also hybridization within cells of the dorsal root ganglion and somites. These signals are above background but

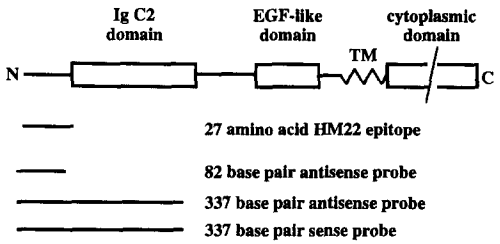

Figure 1. Schematic representation of the ARIA protein sequence compared with the sequences of various probes employed in this study.

less intense than in the spinal cord. At this age (E5), we also found high levels of ARIA mRNA in other regions of the nervous system and the heart (an extensive analysis of ARIA expression in the CNS was reported by Corfas et al., 1995). Expression in the ventral spinal cord persists throughout embryonic development and the amount of ARIA specific mRNA is maintained at similar levels, as judged by autoradiographic exposure times. At the time of hatching, individual motor neuron nuclei may be identified as expressing high levels of ARIA message (Fig. 2, *c* and *d*). A 337-bp sense probe gave background levels of hybridization at all ages studied (data not shown).

Characterization of Anti-ARIA Antiserum

Our success in detecting ARIA mRNA in motor neurons with even quite short NH_2-terminal probes encouraged us to develop antibodies specific for this region to study the distribution ARIA proteins that contain an NH_2-terminal Ig domain. A polyclonal antiserum, called HM22, was raised against a peptide representing the 27 NH_2-terminal amino-acids predicted from the λ12 clone of chick pro-ARIA1 (Fig. 1). The specificity of affinity purified HM22 antiserum was tested by Western blot analysis of ARIA expressed in COS cells. HM22 recognizes a major band at a MW of ~80-kD in extracts of COS cells transfected with ARIA (Fig. 3, lane *2*) that is absent in control preparations of COS cells transfected with a control plasmid (Fig. 3, lane *1*). The size of this band is consistent with the 626–amino acid ARIA construct used (λ12 plus epitope tag), taking into account glycosylation (Falls et al., 1993) and is comparable to the 85-kD band detected with a rat-specific anti-ARIA antibody after COS cells were transfected with the equivalent rat ARIA construct (Sandrock et al., 1995). The binding of HM22 was completely blocked by preincubation with the cognate peptide antigen (Fig. 3, lane *4*). The ARIA construct included a "flag" epitope tag positioned at the amino terminus. Western blots probed with M2, a flag sequence-specific antibody, confirmed that the 80-kD protein was encoded by the transfected ARIA construct (Fig. 3, lane *6*) and thus confirmed that HM22 recognizes ARIA. A second less abundant ARIA species of high molecular mass was specifically labeled with both HM22 and M2 antibodies, although its precise identity remains unknown. Western blot analysis of E19 chick ALD

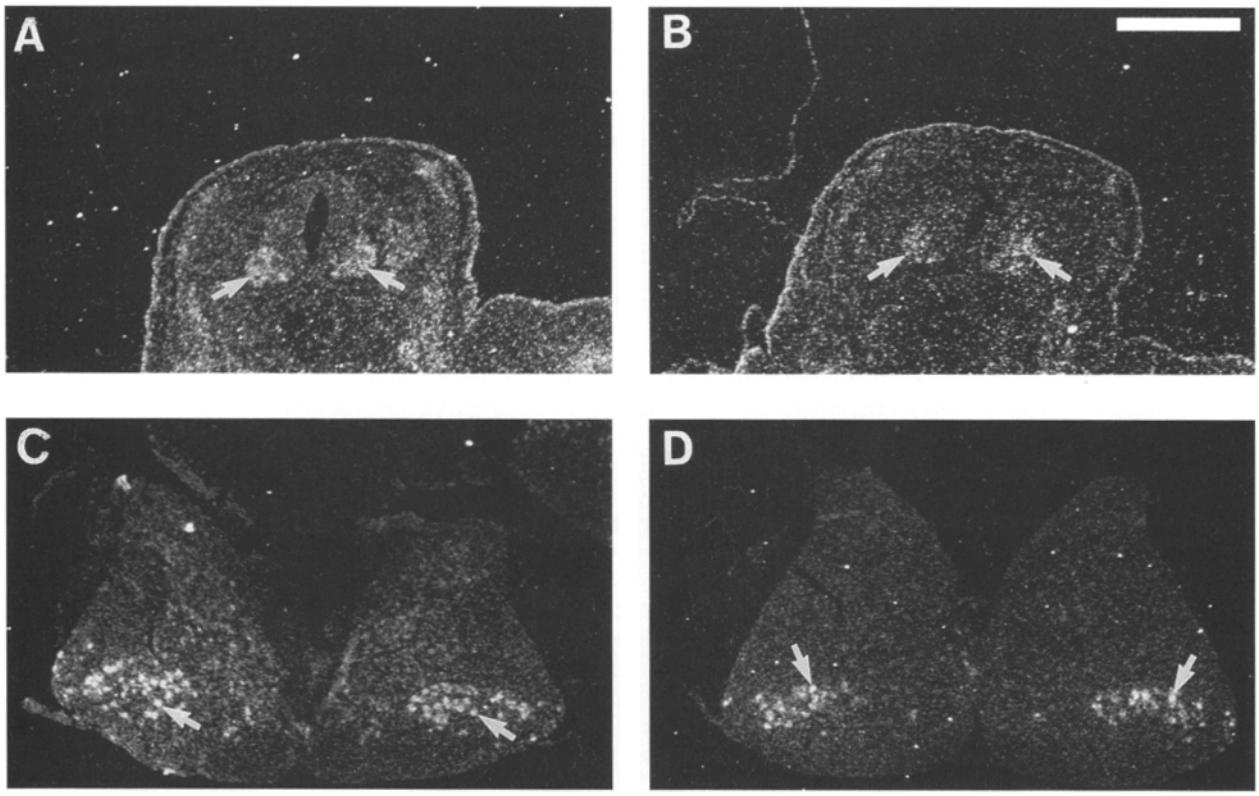

Figure 2. ARIA mRNA is expressed in early (E5) and late (E21) embryonic chick motor neurons. Sections of E5 (*a* and *b*) embryo and E21 (*c* and *d*) spinal cord were incubated with either 82 (*a* and *c*) or 337 bp (*b* and *d*) RNA antisense probes specific for the NH_2 terminus of ARIA. Elevated ARIA expression in the E5 ventral spinal cord (*arrows*) coinciding with newly differentiated motor neurons is evident with both probes (*a* and *b*). By E21, individual highly expressing motor neuron nuclei (*arrows*) may clearly be identified (*c* and *d*). Bar: (*a* and *b*) 300 μm; (*c* and *d*) 500 μm.

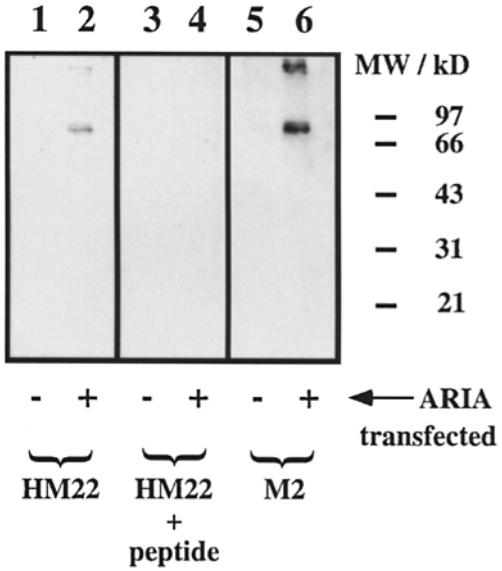

Figure 3. Specific binding of affinity-purified HM22 polyclonal antibodies to COS cell-expressed flag epitope-tagged ARIA detected by immunoblot. Extracts of COS cells, transfected either with the p12.6 antisense control vector (lanes *1*, *3*, and *5*) or a vector including sequence encoding ARIA tagged with the flag epitope (Euflag1), were run on SDS-PAGE and electroblotted to PVDF membrane (lanes *2*, *4*, and *6*). Membranes were incubated with HM22 anti-ARIA antibody in the absence (lanes *1* and *2*) or presence (lanes 3 and *4*) of peptide antigen. As a positive control, transfected ARIA protein was identified using the M2 anti-flag monoclonal antibody (lanes *5* and *6*). HM22 and M2 antibodies specifically recognize the 80-kD species predicted from the cDNA sequence (lanes *2* and *6*). Both antibodies also detect a high molecular mass ARIA species that barely enters the polyacrylamide gel and probably represents a covalent ARIA aggregate.

muscle showed labeling of several protein bands (data not shown). However, only one HM22 positive band (MW = 45 kD) was absent when the HM22 antibody was preincubated with peptide antigen, a size consistent with brain-purified ARIA (Falls et al., 1993).

ARIA Protein Expression at the Chick nmj

We established fixation conditions using COS/CHO cells transfected with the flag-tagged ARIA construct (see Materials and Methods), and subsequently applied them to localize ARIA in late embryonic chick muscle. We selected the ALD muscle because its fibers are multiply innervated and the large number of regularly spaced nmjs allowed us to examine many endplates in each section. The staining pattern of affinity-purified HM22 on E18 chick ALD muscle, illuminated by indirect immunofluorescence, reveals intense arcs of HM22 staining that are characteristic of chick nmjs at this stage of development (Fig. 4 *a*). This was confirmed by double staining with rhodamine-conjugated α-bungaroxin (Fig. 4 *b*), which irreversibly binds to the clustered ACh receptors at nmjs. All α-bungarotoxin sites were HM22 positive. The specificity of the HM22 binding pattern was confirmed by preincubation of this antibody with peptide antigen. The staining at the nmj quantitatively disappeared in the presence of the peptide (Fig. 4, *c* and *d*). Therefore ARIA is present at all synapses examined in the ALD. In addition, ARIA-like immunoreactivity was found in every other muscle examined including the fast posterior latissimus dorsi and pectoralis muscles.

To maximize the chance of observing extended lengths of preterminal axons immediately proximal to nmjs, we labeled longitudinal sections of ALD muscles (Fig. 5 *a*). In this orientation, the nmjs form a line beneath the motor nerve, which lies across the muscle fiber (Fig. 5 *b*). The size and shape of the ARIA staining pattern, revealed by HM22, corresponds well with that of α-bungarotoxin–labeled AChRs seen en face in this orientation. In contrast, ARIA protein could not be detected along the axon: the HM22 staining pattern (Fig. 5 *a*) was not coextensive with that of the 160-kD neurofilament protein (Fig. 5 *b*). Also, we were unable to detect ARIA-like immunoreactivity with HM22 in motor neuron cell bodies in transverse sections of the lumbar and cervical spinal cord (data not shown). We cannot exclude the possibility that Ig-containing ARIA isoforms are present at very low levels in these regions of motor neurons. However, the finding that ARIA protein accumulates only at the endplate supports the hypothesis that ARIA is involved in the development and maintenance of the synapse in vivo.

Developmental Expression of ARIA

The expression of ARIA at ALD muscle endplates was examined during development on embryonic days E5, 8, 10, 12, 14 (data not shown), 15, 16, and 17 (Fig. 6). Despite numerous attempts using a range of fixation and staining conditions, we did not observe ARIA-like immunoreactivity at nmjs on or before E15, when patches of AChRs are clearly present (Fig. 6, *a* and *b*) and functional chick nerve–muscle synapses have been detected in ALD muscles (Bennett and Pettigrew, 1974). One day later (E16), all nmjs are labeled (Fig. 6 *c*), although apparently less intensely than at E17 (Fig. 6 *e*) and later stages. These observations do not eliminate the possibility that there may be low levels of functional ARIA present at or before E15. However, the dramatic and apparently synchronous appearance of ARIA-like immunoreactivity in many hundreds of endplates suggests that it is a tightly regulated process and probably reflects a rapid increase in the synaptic ARIA concentration.

ARIA Is Concentrated in the Synaptic Cleft

To define the location of ARIA at the nmj more precisely, ALD endplates were studied at the electron microscope level. Vibratome sections were incubated with HM22 antibodies and developed using the HRP-ABC method (Hsu et al., 1981). After osmication and embedding in epon/araldite, grazing 65-nm sections were cut across the surface of the vibratome sections. The insoluble HRP reaction product filled the synaptic cleft at every nmj identified (Fig. 7 *a*, *between arrows*). The stain filled the cleft evenly and was present throughout the thickened basal lamina characteristic of the synaptic zone, including the perisynaptic Schwann cell/muscle interface at the margins of the synaptic cleft. In some sections, the perisynaptic Schwann cell capping the nerve terminal extended a significant distance on either side along the muscle surface (Fig. 7 *b*). In-

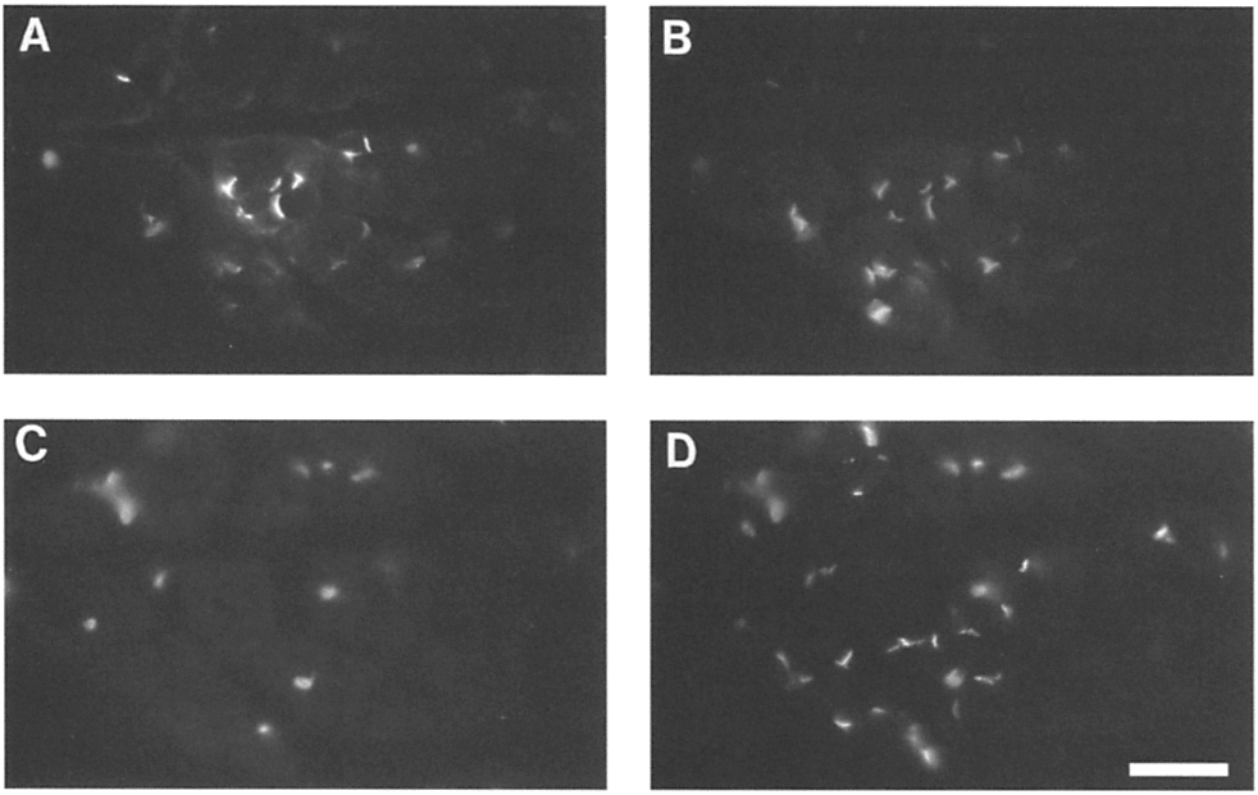

Figure 4. Immunohistological detection of ARIA immunoreactivity at E18 embryonic neuromuscular junctions. Transverse sections of E18 ALD muscle were double labeled with rhodamine-conjugated α-bungarotoxin and HM22 anti-ARIA antibody labeled with fluorescein-conjugated goat anti–rabbit IgG secondary antibodies and illuminated either with fluorescein (*a* and *c*) or rhodamine (*b* and *d*) optics. The section illustrated in the lower panels was incubated with HM22 that had been preincubated with an excess of peptide antigen. The small number of features apparent after peptide blocking of HM22 staining in *c* represent nonspecific autofluorescence from erythrocytes. Bar, 30 μm.

tense ARIA immunoreactivity was continuous in the cleft beneath both Schwann cell and nerve terminal but did not extend beyond the synaptic zone defined by the end of the Schwann cell processes. In occasional sections, low levels of staining on the muscle basal lamina a short distance beyond the Schwann cell were apparent.

Since the sections for electron microscopy were cut from the surface of vibratome sections, the cytoplasm was freely accessible to all antibodies and staining reagents. Despite this exposure, no intracellular staining was evident in muscle, nerve or Schwann cells (Fig. 7, *a* and *b*). Subcellular organelles and vesicles were also unstained, but since detergent that would have permeabilized these structures was not used, we are unable to conclude that ARIA was absent from them.

The HM22 epitope is present in the extracellular domain of the membrane bound proARIA precursor protein as well as in soluble ARIA released from motor neurons. It is unlikely that ARIA is associated solely with the presynaptic nerve cell plasma membrane, as the synaptic ARIA staining includes extensive regions where there is no direct apposition between vesicle-filled nerve terminals and the basal lamina on the muscle surface (Fig. 7 *b*). ARIA staining was absent from the extra-synaptic basal lamina of muscle and the nonsynaptic basal lamina of Schwann cells (Fig. 7, *a* and *b*). No axonal ARIA labeling was apparent intracellularly or on the axolemma (Fig. 7 *a*). Thus even at high resolution, ARIA-like immunoreactivity appears restricted to the synaptic basal lamina.

Further evidence for ARIA association with the basal lamina at the electron microscope level was obtained using immunogold labeling methods. In this technique, ultrathin cryosections were labeled with HM22 and colloidal gold-labeled protein A. We identified nmjs by a combination of criteria including the: (*a*) increased density beneath the sarcolemma, (*b*) thickened basal lamina, (*c*) presence of synaptic vesicle profiles, and (*d*) electron dense cytoplasm of perisynaptic Schwann cell processes. The gold-labeled protein A formed a dense layer in the synaptic basal lamina of muscle cells at many endplates identified by these criteria, confirming the observation that this region contains highly concentrated ARIA (Fig. 8 *a*). As was seen with the HRP labeling technique, no ARIA immunoreactivity was apparent in extra-synaptic regions of muscle basal lamina (Fig. 8 *a*, *open arrow*). In contrast with the HRP stain, which uniformly filled the cleft, the colloidal gold label was not evenly distributed across the basal lamina. Rather, it is largely confined to the surface of the electron dense layer of the lamina on the presynaptic side (Fig. 8 *b*). The labeling extends for the length of the thickened basal lamina including areas of Schwann cell-myotube contact where no nerve terminals are apparent (Fig. 8 *a*, *arrowhead*). This clearly demonstrates that ARIA is localized within the basal lamina, although it does not exclude

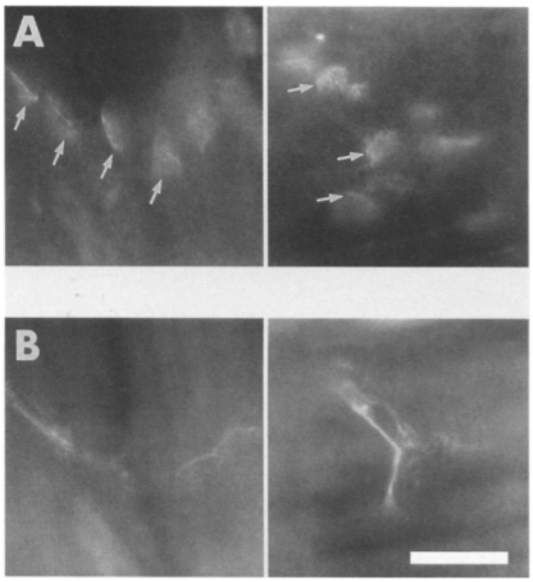

Figure 5. ARIA immunoreactivity is not detectable in motor axons identified with anti neurofilament antibodies. Longitudinal sections of E18 ALD muscle were double labeled with HM22 anti-ARIA antibodies and monoclonal antibodies specific for 160-kD neurofilament protein followed by fluorescein-labeled goat anti–rabbit and rhodamine-labeled goat anti–mouse secondary antibodies and illuminated with fluorescein optics (*a*) or rhodamine (*b*) optics. A succession of HM22 immunoreactive nmjs are seen en face (*a*, *arrows*) along the path of neurofilament labeled motor axons (*b*) that appear to be HM22 negative (*a*). Bar, 30 μm.

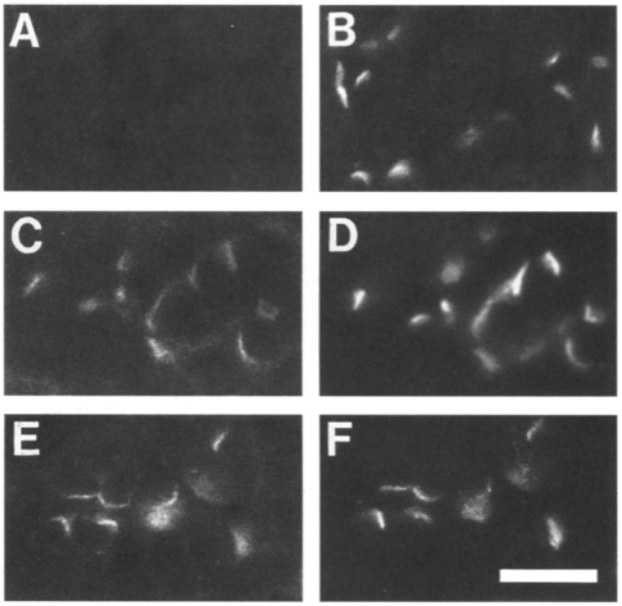

Figure 6. Comparison of HM22 labeling at nmjs at embryonic days 15 (*a* and *b*), 16 (*c* and *d*), and 17 (*e* and *f*). Transverse sections of ALD muscle were double labeled with rhodamine-conjugated α-bungarotoxin and HM22 anti-ARIA antibody labeled with fluorescein-conjugated goat anti–rabbit IgG secondary antibodies and illuminated either with fluorescein (*a*, *c*, and *e*) or rhodamine (*b*, *d*, and *f*) optics. ARIA immunoreactivity is not detectable at E15 (*a*) but is clearly present at all α-bungarotoxin labeled nmjs on E16 and E17 (*c* and *e*). Bar, 30 μm.

the possibility that it may also be associated with the presynaptic nerve terminal plasma membrane. However, the relative uniformity of labeling along the entire length of the cleft argues against concentration in the nerve terminal membrane. Also, we did not detect any labeling associated with presynaptic plasma membrane that had become separated from the basal lamina during sample preparation. In different sections, a range of immunogold labeling densities were seen, including a few junctions where we could not be convinced of above background labeling. We do not yet know if this represents heterogeneity between synapses or reflects the variability inherent in this technique.

An added benefit of colloidal gold labeling was that antibody incubations were carried out directly on 70–80-nm cryosections, allowing the reagents access to all intracellular compartments. Although nerve terminals were incompletely preserved, many presynaptic vesicle profiles were positively identified (Fig. 8 *b*, *curved arrows*) and in other sections we were able to detect significant concentrations of a synaptic vesicle antigen (SV2) associated with these structures (data not shown). These vesicles were not labeled with HM22-associated gold particles (Fig. 8 *b*). In occasional sections, we have seen a few such gold particles at synaptic vesicles but at densities close to background and at levels far less than SV2 labeling. This result, in contrast to that obtained with the HRP method, allows us to conclude that if ARIA is present in synaptic vesicles, its concentration is relatively low. Physiologically, this may reflect the use of an alternate mode of ARIA secretion at the nerve terminal. In summary, our immunoelectron microscopy study demonstrates that Ig containing ARIA is concentrated in the synaptic basal lamina of embryonic chick neuromuscular junctions.

Discussion

In this study, we used riboprobes and polyclonal antibodies specific for the isoforms of ARIA that contain an Ig domain to characterize their expression and distribution in motor neurons and at motor endplates in chick embryos. We found that ARIA mRNA is present in motor neurons at the earliest stages of synaptogenesis and that high levels of expression are then seen throughout embryogenesis. Further, ARIA-like immunoreactivity was found to be concentrated in the basal lamina of the synaptic cleft. These observations are consistent with the model that ARIA is synthesized and secreted by motor neurons. Although we were not able to confirm that ARIA is present within the nerve terminals, several lines of evidence indicate that the ARIA protein within the synaptic cleft is nerve derived. First, there is strong ARIA mRNA expression in motor neurons. Our in situ hybridization studies in the chick have detected ARIA mRNA in all motor neurons from E5 onwards throughout embryogenesis. These studies failed to detect significant hybridization in muscle tissue, another possible source of ARIA in the cleft. Comparative studies that assessed ARIA mRNA expression by Northern blot analysis have also demonstrated significant levels of ARIA mRNA in spinal cord and brain but again not in muscle (Holmes et al., 1992; Wen et al., 1992, 1994).

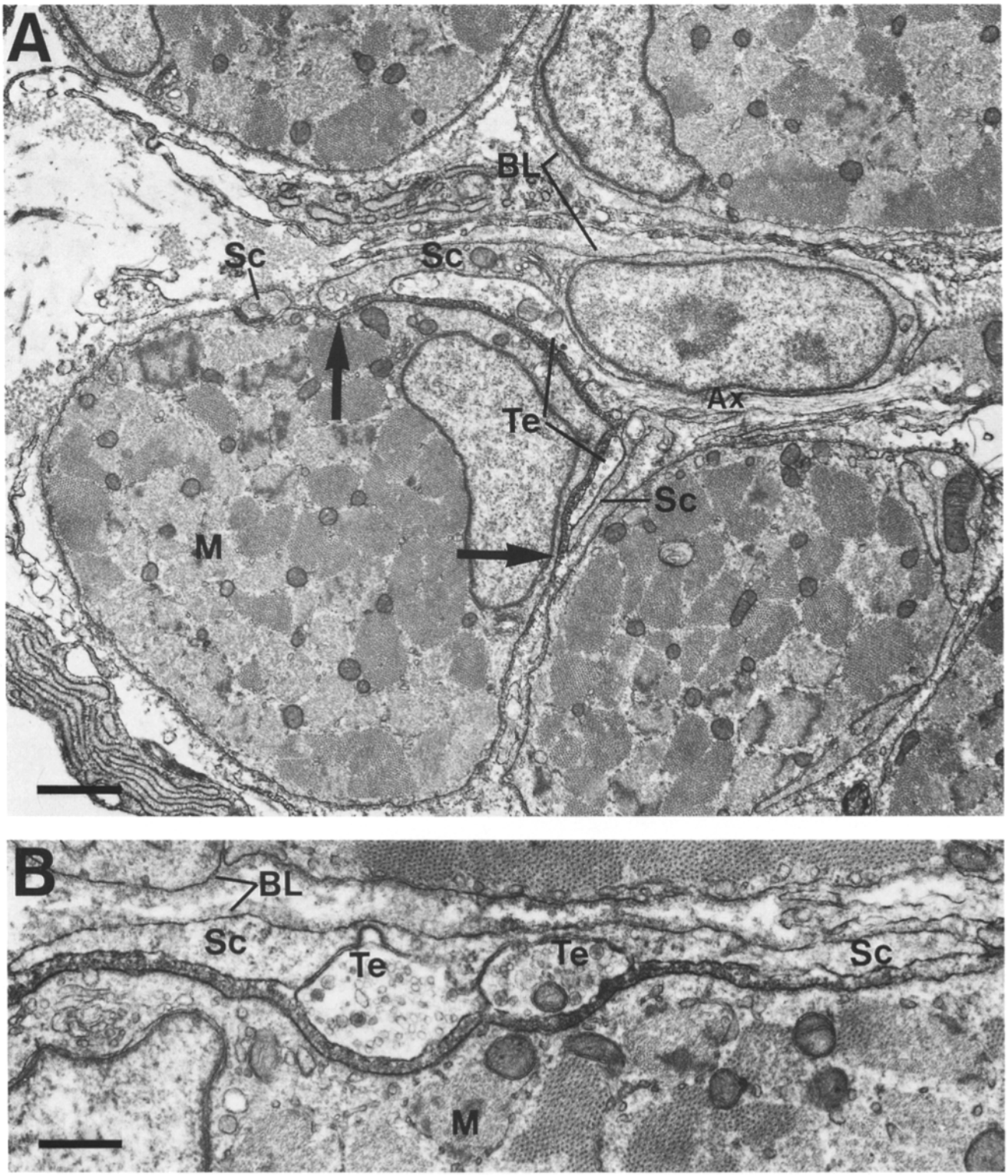

Figure 7. Transmission electron micrographs of E18 chick ALD neuromuscular junctions labeled with HM22 anti-ARIA antibodies. (*a*) The ARIA/HM22 complex was illuminated using the HRP-ABC stain with DAB as a substrate. The resulting dark precipitate was seen only in the synaptic cleft, indicated by the arrows. The nonsynaptic basal laminae (*BL*) of muscle and Schwann cells were unstained. No cytoplasmic staining was evident within the nerve axon (*Ax*), nerve terminal (*Te*), Schwann cell (*Sc*) or muscle (*M*). (*b*) A section at higher magnification, immunolabeled as above, showing extensive ARIA staining between the perisynaptic Schwann cell and muscle surface in addition to that seen immediately beneath the nerve terminal. The absence of stain in the nonsynaptic basal lamina of the Schwann cell and an adjacent muscle cell is particularly evident in this section. Bars: (*a*) 0.5 μm; (*b*) 0.25 μm.

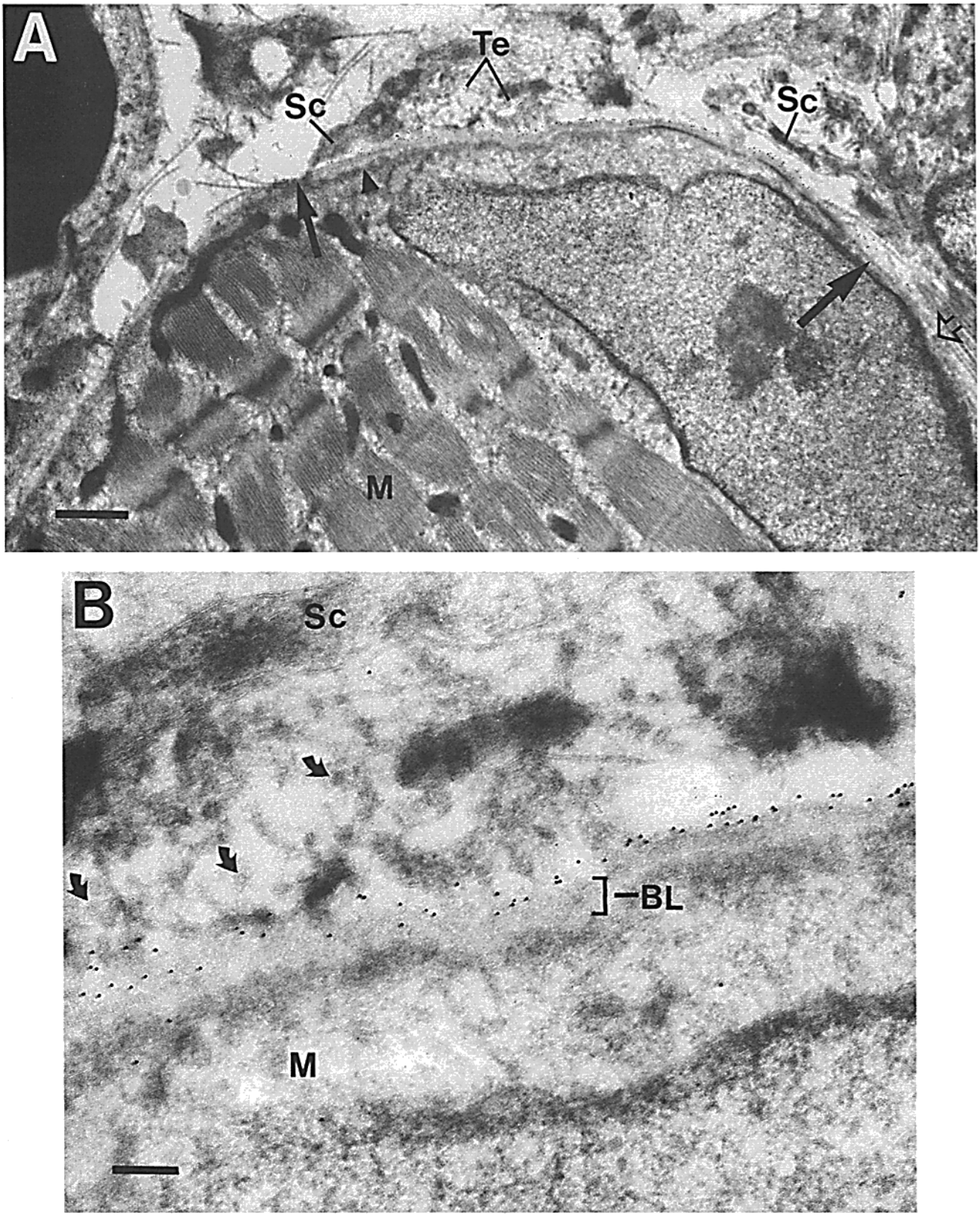

Figure 8. Immunogold staining with HM22 anti-ARIA antibodies on ultrathin cryosections of E18 chick ALD muscle. (*a*) The ARIA/HM22 complex is labeled by protein A-conjugated 10-nm colloidal gold particles that are present at high density throughout the synaptic cleft (*between filled arrows*). The arrowhead indicates a labeled region between a perisynaptic Schwann cell and the muscle surface. The open arrow indicates a region of unlabeled muscle basal lamina. (*b*) A detail of *a* is further magnified to show that the gold label is almost exclusively restricted to the outer surface of the basal lamina (*BL*). Curved arrows show examples of synaptic vesicles within the nerve terminal that are unlabeled. Schwann cell (*Sc*), nerve terminal (*Te*), and muscle cell (*M*) are indicated. Bars: (*a*) 0.2 μm; (*b*) 0.1 μm.

Second, evidence that ARIA is secreted by motor neurons has been obtained from assays of ARIA activity in cell culture. When myotubes were cultured in the presence of medium conditioned by purified embryonic chick motor neurons, the rate of AChR incorporation increased and p185, the putative ARIA receptor (Corfas et al., 1993; Falls et al., 1993), was rapidly and specifically phosphorylated on tyrosine residues. In contrast, no such activity was detected in medium conditioned by embryonic muscle cell cultures. Third, we have observed an acute decrease in ARIA-like immunoreactivity at adult rat nmjs within 2 d of denervation (Sandrock et al., 1995). The Schwann cell capping the nerve cell is another potential source of ARIA protein in the synaptic cleft, although no significant in situ hybridization with either riboprobe used in this study was observed in muscle. In summary, the weight of evidence suggests that ARIA protein at the nmj is nerve derived, although the possibility that muscle or Schwann cells are a source of ARIA cannot be fully excluded.

The absence of significant ARIA immunoreactivity in spinal cord motor neuron cell bodies, compared with the high level of mRNA expression, suggests that the combined rates of transport and degradation of ARIA protein are equal to or greater than the rate of ARIA protein synthesis, leading to little accumulation of ARIA within the cell soma. From the high levels of ARIA protein that we observe at motor nerve terminals, we conclude that nascent ARIA is rapidly transported from the cell body down the axon and released at the end plate. Precedent for this phenomenon has been set by other motor neuron proteins, including the synaptic vesicle protein SV2 that is present at high concentrations in motor nerve terminals but is undetectable in motor neuron cell bodies (Buckley and Kelly, 1985). Direct evidence that ARIA is transported away from the motor neuron cell body has also recently been obtained: ARIA-like immunoreactivity appears in proximal motor axons when axonal transport is blocked by colchicine (Sandrock et al., 1995). Rapid axonal transport would be consistent with our observation that ARIA protein is highly concentrated at the nerve terminal. Furthermore, localization of ARIA to the nmj fulfills a key prerequisite of its proposed role as a trophic factor that acts on muscle.

We have observed high levels of ARIA-like immunoreactivity in the synaptic cleft using electron microscopy with both HRP and immunogold labeling techniques. However, we were unable to detect significant levels within the nerve terminals either in vesicles or in the cytoplasm. If ARIA were free to diffuse after release, its extracellular concentration would be at or below that within the nerve. The intense labeling that we observe is therefore evidence that ARIA becomes trapped within the synaptic cleft. This entrapment is unlikely to be a nonspecific physical effect, as proteins much larger than ARIA, such as ferritin whose molecular mass is more than 10 times greater than that of ARIA, rapidly diffuse within the synaptic cleft (Oldfors and Fardeau, 1983). Thus the concentration of ARIA within the cleft is likely to be due to specific molecular interactions.

ARIA immunoreactivity was detected between the muscle and perisynaptic Schwann cell as well as immediately beneath nerve terminals. The fact that ARIA immunoreactivity was restricted to the basal lamina of the synaptic zone and that it was found almost exclusively on the presynaptic part of the lamina would support the hypothesis that the distribution of ARIA is determined by the distribution of one or more components of the basal lamina with which it interacts. If so, it follows that the appearance of the intense ARIA-like immunoreactivity in the synaptic cleft between E15 and E16 may be determined by the accumulation of the ARIA-binding molecules. Lower but biologically active concentrations of ARIA may be present at the synapse earlier, when AChR clusters are first observed. This view is supported further by in vitro studies where ARIA activity was detected in medium conditioned by chick motor neurons as early as E8 (data not shown). Whether secretion arises as soon as ARIA mRNA is detected at E5 has yet to be determined.

One class of molecules that may mediate the association of ARIA with the synaptic cleft is heparan sulfate proteoglycans (HSPGs). ARIA is known to interact with heparin in vitro, an affinity that was exploited in several strategies used to purify ARIA family ligands (Holmes et al., 1992; Peles et al., 1992; Falls et al., 1993). Low doses of heparin inhibit the ARIA-dependent autophosphorylation of the p185 ARIA receptor (Loeb and Fischbach, 1995). This effect was not observed with the EGF domain alone, suggesting that the interaction with heparin is mediated by the Ig C2 domain that includes two regions of primary sequence rich in basic residues. Although a HSPG is heavily concentrated at the nmj (Sanes et al., 1986), the sulfated glycosaminoglycan chains are thought to be located mainly in the lamina rara (Kanwar and Farquhar, 1979), an electron lucent layer immediately proximal to the muscle plasma membrane. If HSPGs bind ARIA in vivo, this distribution becomes difficult to reconcile with the concentration of ARIA labeling observed on the presynaptic side of the basal lamina. There are a number of candidates in addition to HSPGs that may mediate ARIA binding to the synaptic basal lamina. Ig C2 domains are contained in many extracellular matrix molecules and have been shown to mediate both homophilic and heterophilic protein/protein interactions (Williams and Barclay, 1988) and some such proteins, including NCAM for example (Sanes et al., 1986), are specifically concentrated in the synaptic basal lamina. Direct measurement of ARIA-binding affinities of such candidate proteins coupled to further electron microscopy studies on their distribution in the synaptic basal lamina promise to define ARIA's molecular-binding partners in the synaptic cleft.

ARIA is synthesized as a precursor with a single transmembrane region dividing cytoplasmic and extracellular domains. The extracellular domain is released through proteolytic cleavage and may be processed further (Loeb and Fischbach, 1995). These different forms occupy discrete extracellular compartments, and may perform different functions according to their distinct distribution. The dramatic appearance of ARIA-like immunoreactivity between E15 and E16 and the persistence of this staining until hatching and into adulthood suggests that basal lamina-associated ARIA is likely to be involved in the maturation and maintenance of synapses. During the latter part of gestation, the number of AChRs on the muscle surface drops dramatically while receptors beneath the motor

endplates remain. These receptor patches enlarge until the synaptic density is as much as 10,000 times greater than that found extrasynaptically (Fertuck and Salpeter, 1976). Release of ARIA from the synaptic basal lamina, either by dissociation or proteolysis (Loeb and Fischbach, 1995), might be necessary to effect AChR synthesis at the level required to maintain this extreme density.

The concentration of ARIA within the cleft between E15 and E16 may be important for the regulation of synaptic molecules other than AChRs. For example, ARIA has been shown to increase the number of sodium channels on the surface of cultured muscle cells (Corfas and Fischbach, 1993). In addition, the concentration of ARIA within the synaptic cleft could also effect changes in perisynaptic Schwann cells that are present as early as E8 (Atsumi, 1977), particularly if, like axonal Schwann cells, they possess receptors for ARIA family ligands (Marchionni et al., 1993).

Basal lamina-associated ARIA may also function in maintaining the integrity of synapses during tissue regeneration after nerve injury. After nerve crush, motor neurons regrow down the path of the degenerating nerve and reinnervate their target muscle at the original synaptic site (Marshall et al., 1977). Evidence has been presented that demonstrates that a nerve-derived basal lamina constituent (or constituents) maintains synapse-specific AChR expression in the muscle at the site of the original nmj during nerve regeneration (Burden et al., 1979; Goldman et al., 1991; Brenner et al., 1992; Jo and Burden, 1992). Basal lamina-associated ARIA is clearly a strong candidate to regulate AChR expression in the absence of functional innervation. This hypothesis is strengthened by the observation that reduced but significant levels of ARIA-like immunoreactivity persist at nmjs after denervation (Jo et al., 1995; Sandrock et al., 1995). Confirmation of the role of ARIA in the maintainance and repair of the synapse awaits the development of reagents that are able to perturb ARIA's function over extended periods of time in vivo.

This study focused on members of the ARIA ligand family that possess an NH_2-terminal Ig C2 domain because these isoforms were the first to be purified and are abundantly represented in cDNA libraries prepared from diverse sources (Marchionni et al., 1993; Wen et al., 1994). However, there are two classes of alternative splice variants that we did not detect: those that possess different NH_2-terminal regions and thus no HM22 epitope. One is the "GGF2" class whose cDNAs encode a 245-amino acid domain of unknown function spliced at the NH_2 terminus of the Ig C2 domain in place of the HM22 epitope (Marchionni et al., 1993). Although no "GGF2" sequences have been reported in the chick, using S1 nuclease protection we have identified a splice junction in embryonic chick spinal cord mRNA that is consistent with the presence of the GGF2 isoform (Rosen, K. M. and G. D. Fischbach, unpublished results). Secondly, cDNAs have been identified in embryonic spinal cord where, in place of the Ig domain, an entirely unrelated NH_2-terminal domain is spliced to the EGF-like domain (Kuo, Y., X. Yang, and L. Role. 1994. Society for Neuroscience Annual Meeting. Abstract 452.18; Ho et al., 1995). Thus we have identified a subset of ARIA isoforms at the neuromuscular junction that extends observations made in parallel by other groups who found ARIA-like immunoreactivity at adult mammalian nmjs using antibodies that did not distinguish between different members of the ARIA ligand family (Chu et al., 1995; Jo et al., 1995).

As discussed above, it is likely that the Ig C2 domain plays a role in the interaction of ARIA with the synaptic basal lamina. This may represent a more general function of NH_2-terminal domains acting as determinants of the extracellular distribution of members of this ligand family and thus for presenting the bioactive EGF-like domain to target cells. This hypothesis is consistent with a preliminary report that GGF2 NH_2-terminal domain-specific immunoreactivity is present in adult rat motor axons but not at nerve terminals (Jo et al., 1995). A comparison of the distribution of these three classes of ARIA-like ligands in motor neurons at different embryonic ages would be highly informative as to the role of the NH_2-terminal domains in biological function of ARIA.

In this study, we have demonstrated the presence of ARIA protein in the synaptic cleft between nerve and muscle. This is consistent with the hypothesis that ARIA has a trophic-signaling function between these cells. Furthermore we have shown that ARIA is highly concentrated in the synaptic basal lamina, probably as a result of specific binding to other proteins. The stage is now set for examination of ARIA's role in initial events of synaptogenesis and its possibly distinct role at mature synapses by blocking ARIA function in vitro and in vivo.

The authors would like to thank Drs. L. Crews and K. Rosen for critical reading of the manuscript and J. Gagliardi for photographic assistance. COS cell expression vectors were prepared by Drs. D. Falls and E. Lieth. Synthetic peptides were prepared at the Howard Hughes Medical Institute Biopolymer Facility by Dr. J. Rush.

This work was supported in part by grants from National Institutes of Health (R01-8226), and fellowships from the Massachusetts Medical Foundation (G. Corfas) and the Harvard Mahoney Neuroscience Institute (A. Goodearl).

Received for publication 19 May 1995 and in revised form 29 June 1995.

References

Atsumi, S. 1977. Development of neuromuscular junctions of fast and slow muscles in the chick embryo: a light and electron microscopic study. *J. Neurocytology.* 6:691–709.

Bennett, M. R., and A. G. Pettigrew. 1974. The formation of synapses in striated muscle during development. *J. Physiol.* 241:515–545.

Bennett, M. R., D. F. Davey, and K. E. Uebel. 1980. The growth of segmental nerves from the brachial myotomes into the proximal muscles of the chick forelimb during development. *J. Comp. Neurol.* 189:335–357.

Bonner, P. H., and S. D. Hauschka. 1974. Clonal analysis of vertebrate myogenesis. I. Early developmental events in the chick limb. *Dev. Biol.* 37:317–328.

Brenner, H. R., A. Herczeg, and C. R. Slater. 1992. Synapse-specific expression of acetylcholine receptor genes and their products at original synaptic sites in rat soleus muscle fibres regenerating in the absence of innervation. *Development (Camb.).* 116:41–53.

Buckley, K., and R. B. Kelly. 1985. Identification of a transmembrane glycoprotein specific for secretory vesicles of neural and endocrine cells. *J. Cell Biol.* 100:1284–1294.

Burden, S. J., P. B. Sargent, and U. J. McMahan. 1979. Acetylcholine receptors in regenerating muscle accumulate at original synaptic sites in the absence of the nerve. *J. Cell Biol.* 82:412–425.

Chu, G. C., L. M. Moscoso, M. X. Sliwkowski, and J. P. Merlie. 1995. Regulation of the acetylcholine receptor epsilon subunit gene by recombinant ARIA—an in vitro model for transynaptic gene regulation. *Neuron.* 14:329–339.

Corfas, G., and G. D. Fischbach. 1993. The number of Na^+ channels in cultured chick muscle is increased by ARIA, an acetylcholine receptor-inducing activity. *J. Neurosci.* 13:2118–2125.

Corfas, G., D. L. Falls, and G. D. Fischbach. 1993. ARIA, a protein that stimu-

lates acetylcholine receptor synthesis, also induces tyrosine phosphorylation of a 185-kDa muscle transmembrane protein. *Proc. Nat. Acad. Sci. USA.* 90: 1624–1628.

Corfas, G., K. M. Rosen, H. Aratake, R. Krauss, and G. D. Fischbach. 1995. Differential expression of ARIA isoforms in the rat brain. *Neuron.* 14:103–115.

Dubinsky, J. M., D. J. Loftus, G. D. Fischbach, and E. L. Elson. 1989. Formation of acetylcholine receptor clusters in chick myotubes: migration or new insertion? *J. Cell Biol.* 109:1733–1743.

Fallon, J. R., and C. E. Gelfman. 1989. Agrin-related molecules are concentrated at acetylcholine receptor clusters in normal and aneural developing muscle. *J. Cell Biol.* 108:1527–1535.

Fallon, J. R., and Z. W. Hall. 1994. Building Synapses—agrin and dystroglycan stick together. *Trends Neurosci.* 17:469–473.

Falls, D. L., K. M. Rosen, G. Corfas, W. S. Lane, and G. D. Fischbach. 1993. ARIA, a protein that stimulates acetylcholine receptor synthesis, is a member of the neu ligand family. *Cell.* 72:801–815.

Fertuck, H. C., and M. M. Salpeter. 1976. Quantitation of junctional and extrajunctional acetylcholine receptors by electron microscope autoradiography after ^{125}I-alpha-bungarotoxin binding at mouse neuromuscular junctions. *J. Cell Biol.* 69:144–158.

Frank, E., and G. D. Fischbach. 1979. Early events in neuromuscular junction formation in vitro: induction of acetylcholine receptor clusters in the postsynaptic membrane and morphology of newly formed synapses. *J. Cell Biol.* 83:143–158.

Goldman, D., B. M. Carlson, and J. Staple. 1991. Induction of adult-type nicotinic acetylcholine receptor gene expression in noninnervated regenerating muscle. *Neuron.* 7:649–658.

Goodearl, A. D., J. B. Davis, K. Mistry, L. Minghetti, M. Otsu, M. D. Waterfield, and P. Stroobant. 1993. Purification of multiple forms of glial growth factor. *J. Biol. Chem.* 268:18095–18102.

Hall, Z. W., and J. R. Sanes. 1993. Synaptic structure and development: the neuromuscular junction. *Cell.* 72 (Suppl.):99–121.

Harris, D. A., D. L. Falls, D. R. Dill, and G. D. Fischbach. 1988. Acetylcholine receptor-inducing factor from chicken brain increases the level of mRNA encoding the receptor alpha subunit. *Proc. Nat. Acad. Sci. USA.* 85:1983–1987.

Ho, W.-H., M. P. Armanini, A. Nuijens, H. Phillips, and P. L. Osherhoff. 1995. Sensory and motor neuron-derived factor: a novel heregulin variant highly expressed in sensory and motor neurons. *J. Biol. Chem.* 270:14523–14532.

Holmes, W. E., M. X. Sliwkowski, R. W. Akita, W. J. Henzel, J. Lee, J. W. Park, D. Yansura, N. Abadi, H. Raab, G. D. Lewis, et al. 1992. Identification of heregulin, a specific activator of p185erbB2. *Science (Wash. DC).* 256:1205–1210.

Hopp, T. P., K. S. Prickett, V. Price, R. T. Libby, C. J. March, P. Cerretti, D. L. Urdal, and P. J. Conlon. 1988. A short peptide marker sequence useful for recombinant protein identification and purification. *Biotechnology.* 6:1205–1210.

Hsu, S. M., L. Raine, and H. Fanger. 1981. The use of antiavidin antibody and avidin-biotin-peroxidase complex in immunoperoxidase technics. *Am. J. Clin. Pathol.* 75:816–821.

Jo, S. A., and S. J. Burden. 1992. Synaptic basal lamina contains a signal for synapse-specific transcription. *Development (Camb.).* 115:673–680.

Jo, S. A., X. J. Zhu, M. A. Marchionni, and S. J. Burden. 1995. Neuregulins are concentrated at nerve-muscle synapses and activate ACh-receptor gene expression. *Nature (Lond.).* 373:158–161.

Kanwar, Y. S., and M. G. Farquhar. 1979. Anionic sites in the glomerular basement membrane. In vivo and in vitro localization to the laminae rarae by cationic probes. *J. Cell Biol.* 81:137–153.

Landmesser, L. 1978. The development of motor projection patterns in the chick hind limb. *J. Physiol.* 284:391–414.

Landmesser, L., and D. G. Morris. 1975. The development of functional innervation in the hind limb of the chick embryo. *J. Physiol.* 249:301–326.

Loeb, J. A., and G. D. Fischbach. 1995. ARIA can be released from extracellular matrix through cleavage of a heparin-binding domain. *J. Cell Biol.* 130: 127–135.

Marchionni, M. A., A. D. Goodearl, M. S. Chen, M. O. Bermingham, C. Kirk, M. Hendricks, F. Danehy, D. Misumi, J. Sudhalter, K. Kobayashi et al. 1993. Glial growth factors are alternatively spliced erbB2 ligands expressed in the nervous system. *Nature (Lond.).* 362:312–318.

Marshall, L. M., J. R. Sanes, and U. J. McMahan. 1977. Reinnervation of original synaptic sites on muscle fiber basement membrane after disruption of the muscle cells. *Proc. Nat. Acad. Sci. USA.* 74:3073–3077.

Martinou, J. C., D. L. Falls, G. D. Fischbach, and J. P. Merlie. 1991. Acetylcholine receptor-inducing activity stimulates expression of the epsilon-subunit gene of the muscle acetylcholine receptor. *Proc. Nat. Acad. Sci. USA.* 88: 7669–7673.

Oldfors, A., and M. Fardeau. 1983. The permeability of the basal lamina at the neuromuscular junction. An ultrastructural study of rat skeletal muscle using particulate tracers. *Neuropathol. Appl. Neurobiol.* 9:419–432.

Peles, E., S. S. Bacus, R. A. Koski, H. S. Lu, D. Wen, S. G. Ogden, R. B. Levy, and Y. Yarden. 1992. Isolation of the neu/HER-2 stimulatory ligand: a 44 kd glycoprotein that induces differentiation of mammary tumor cells. *Cell.* 69: 205–216.

Ravdin, P., and D. Axelrod. 1977. Fluorescent tetramethyl rhodamine derivatives of alpha-bungarotoxin: preparation, separation, and characterization. *Anal. Biochem.* 80:585–592.

Reist, N. E., M. J. Werle, and U. J. McMahan. 1992. Agrin released by motor neurons induces the aggregation of acetylcholine receptors at neuromuscular junctions. *Neuron.* 8:865–868.

Sandrock, A. W., A. D. J. Goodearl, Q.-W. Yin, D. Chang, and G. D. Fischbach. 1995. ARIA is concentrated in nerve terminals at neuromuscular junctions and at other synapses. *J. Neurosci.* In press.

Sanes, J. R., M. Schachner, and J. Covault. 1986. Expression of several adhesive macromolecules (N-CAM, L1, J1, NILE, uvomorulin, laminin, fibronectin, and a heparan sulfate proteoglycan) in embryonic, adult, and denervated adult skeletal muscle. *J. Cell Biol.* 102:420–431.

Sassoon, D., and N. Rosenthal. 1993. Detection of messenger RNA by in situ hybridization. *Methods Enzymol.* 225:384–404.

Slot, J. W., and H. J. Geuze. 1985. A new method of preparing gold probes for multiple-labeling cytochemistry. *Eur. J. Cell Biol.* 38:87–93.

Smith, M. A., and C. R. Slater. 1983. Spatial distribution of acetylcholine receptors at developing chick neuromuscular junctions. *J. Neurocytol.* 12:993–1005.

Tokuyasu, K. T. 1986. Application of cryoultramicrotomy to immunocytochemistry. *J. Microsc. (Oxford).* 143:139–149.

Tosney, K. W., and L. T. Landmesser. 1985. Development of the major pathways for neurite outgrowth in the chick hindlimb. *Dev. Biol.* 109:193–214.

Usdin, T. B., and G. D. Fischbach. 1986. Purification and characterization of a polypeptide from chick brain that promotes the accumulation of acetylcholine receptors in chick myotubes. *J. Cell Biol.* 103:493–507.

Wen, D., E. Peles, R. Cupples, S. V. Suggs, S. S. Bacus, Y. Luo, G. Trail, S. Hu, S. M. Silbiger, R. B. Levy, et al. 1992. Neu differentiation factor: a transmembrane glycoprotein containing an EGF domain and an immunoglobulin homology unit. *Cell.* 69:559–572.

Wen, D., S. V. Suggs, D. Karunagaran, N. Liu, R. L. Cupples, Y. Luo, A. M. Janssen, B. N. Ben, D. B. Trollinger, V. L. Jacobsen, et al. 1994. Structural and functional aspects of the multiplicity of Neu differentiation factors. *Mol. Cell. Biol.* 14:1909–1919.

Williams, A. F., and A. N. Barclay. 1988. The immunoglobulin superfamily—domains for cell surface recognition. *Annu. Rev. Immunol.* 6:381–405.